

Misalignment mechanism for a mass-varying vector boson

Kunio Kaneta,^a Hye-Sung Lee,^b Jiheon Lee,^b Jaeok Yi^b

^aDepartment of Mathematics, Tokyo Woman's Christian University
Tokyo 167-8585, Japan

^bDepartment of Physics, Korea Advanced Institute of Science and Technology
Daejeon 34141, Korea

E-mail: kkaneta@lab.twcu.ac.jp, hyesung.lee@kaist.ac.kr, anff0101@kaist.ac.kr,
wodhr1541@kaist.ac.kr

Abstract. A coherent field over the entire universe is an attractive picture in studying the dark sector of the universe. The misalignment mechanism, which relies on inflation to achieve homogeneous of the field, is a popular mechanism for producing such a coherent dark matter. Nevertheless, unlike a scalar field case, a vector boson field suffers because its energy density is exponentially suppressed by the scale factor during the cosmic expansion. We show that if the vector field gets a mass from a scalar field, whose value increases by orders of magnitude, the suppression can be compensated, and the misalignment can produce the coherent vector boson that has a sizable amount of energy density in the present universe. Quintessence can be such a scalar field.

Contents

1	Introduction	1
2	Gauged quintessence model	2
3	Dynamics of the gauged quintessence model	4
3.1	Dynamics of the dark gauge boson	4
3.2	Dynamics of the quintessence	6
4	Constraints	9
4.1	Backreaction of ρ_X during the inflation	9
4.2	Isocurvature fluctuation	9
4.3	Stochastic correction to the quintessence evolution	10
5	Summary and discussion	12
A	Extra scenarios	13
B	Growth of the fluctuations	14

1 Introduction

The Λ -CDM model successfully explains many cosmological observational data, including the cosmological microwave background (CMB) spectrum [1]. It consists of ordinary matter, cold dark matter (CDM), and dark energy described by the cosmological constant Λ . Because of its success, it is sometimes called the concordance cosmological model. Nonetheless, the Λ -CDM model bears many questions about its dark components. There have been copious studies about dark matter [2–23], but dark energy remains the vaguest part of the model.

In the Λ -CDM model, the Λ is determined to fit the observational data including the CMB anisotropy [1]. Although this description is simple, it is not satisfying for several reasons. For example, there is no particular reason why the energy density of the cosmological constant is comparable to that of dark matter in the recent era (cosmological coincidence problem) [24]. Also, the distant conjecture on the swampland prefers a dynamically varying vacuum to a constant vacuum [25, 26]. In recent years, the Hubble tension, a 5σ discrepancy between the early universe measurement by Planck [27] and the late universe measurement by SH0ES [28] on the Hubble constant, has emerged as a significant challenge to the Λ -CDM model [29–33]. Since it is a deviation between the experimental data and Λ -CDM model, this tension triggered a sharp increase in dark energy research [34–47]. Therefore, exploring alternatives like quintessence and other dark energy scenarios is warranted.

Quintessence is a dark energy model identifying dark energy as a scalar field slowly rolling down the potential [48–50]. Its dynamics may address the cosmological coincidence problem [51]. Also, the quintessence model can be modified to have some symmetries. For instance, the quintessence is formulated as the gauge field [52–55], associated with the global symmetry [56–64], and Higgs field with a non-abelian gauge symmetry [65–68]. Although the idea of quintessence is very interesting, the minimal quintessence model usually worsens

the Hubble tension [34, 44, 46, 47, 69–74] while a coupled quintessence might give a different result [74, 75].

We suggested the “gauged quintessence” model in the previous work [76]. This model interprets the quintessence as the radial part of a complex scalar charged by a dark Abelian gauge symmetry. The mass of a dark gauge boson, the vector gauge boson corresponding to the dark $U(1)$ symmetry, is given by the value of quintessence. Since the value of quintessence varies in time, the dark gauge boson has a mass-varying characteristic. Unlike the uncoupled quintessence model, the effective equation of state of the dark energy in the gauged quintessence model can be smaller than -1 in the near-past. Due to this fact, the gauged quintessence might relax the drawbacks of quintessence on Hubble tension. Also, recent studies suggest that scenarios containing the couplings between dark energy and dark matter could be a viable solution to Hubble tension [34, 35, 38, 47, 77].

Therefore, it is important to ask “How much relic dark gauge boson could be in the present?” but the answer to this question is non-trivial due to the mass varying characteristic of the dark gauge boson. As a concrete example, we revisit the misalignment [78–81] production of coherent oscillating dark gauge boson [82]. Although the misalignment mechanism is widely used in the scalar case, especially in the axion dark matter production, the misalignment production of a massive vector is extremely difficult. It turned out that a naive model in Ref. [82] cannot produce the sizable relic vector boson because the energy density of the vector boson, unlike the scalar case, exponentially decreases during inflation¹. Alternative models have been proposed to maintain the energy density of the vector boson during inflation. Refs. [84, 86] suggested coupling of the vector boson to Ricci scalar, but it suffers from ghost instability of the longitudinal fluctuation [85]. Refs. [85, 87] suggested coupling to the inflaton, but isocurvature fluctuation and anisotropy of curvature fluctuation restrict the relic density of vector to be much smaller than the dark matter relic density [87].

In this paper, we suggest the misalignment mechanism for producing a sizable amount of the coherent vector boson may work if the vector boson mass increases by many orders of magnitude. We show this with the gauged quintessence model, where the quintessence scalar value and, thus, the vector boson mass increase greatly during the cosmic evolution. The dark gauge boson can achieve a comparable energy density as the CDM.

A brief review of the gauged quintessence model is in Sec. 2. In Sec. 3, we investigate the dynamics of the dark gauge boson from the inflation. In Sec. 4, constraints on gauged quintessence model produced by the misalignment mechanism are discussed, before the summary and discussion in Sec. 5.

2 Gauged quintessence model

The gauged quintessence model [76] includes a complex scalar Φ and a $U(1)_{\text{dark}}$ gauge boson X_μ . The complex scalar is charged under the $U(1)_{\text{dark}}$ gauge symmetry, and consists of the radial part ϕ and the angular part η , $\Phi = \phi e^{i\eta}/\sqrt{2}$. The radial part ϕ is taken as the quintessence field.

Under the unitary gauge,

$$\eta = 0, \quad X_\mu = X_\mu + \frac{1}{g_X} \partial_\mu \eta, \quad (2.1)$$

¹To have a correct relic dark matter density, the mass of a vector boson should be smaller than 10^{-38} GeV, but the Lyman- α forest gives a strong constraint on the relic dark matter density if the mass of a vector is less than 10^{-30} GeV. [83–85]

the action of gauged quintessence model is given by²

$$S \supset \int d^4x \sqrt{-g} \left[-\frac{1}{2}(\partial_\mu \phi)(\partial^\mu \phi) - \frac{1}{4}X_{\mu\nu}X^{\mu\nu} - V_0(\phi) - \frac{1}{2}(g_X \phi)^2 X_\mu X^\mu \right], \quad (2.2)$$

where g_X is the dark gauge coupling constant. The last term in Eq. (2.2) gives the mass of the dark gauge boson, and at the same time, it affects the quintessence dynamics. We call this term the gauge potential:

$$V_{\text{gauge}} = \frac{1}{2}g_X^2 \phi^2 X_\mu X^\mu. \quad (2.3)$$

For the scalar potential $V_0(\phi)$, we take the inverse-power potential (Ratra-Peebles potential) suggested by Ratra and Peebles [49]:

$$V_0(\phi) = \frac{M^{\alpha+4}}{\phi^\alpha}, \quad (2.4)$$

where $\alpha > 0$ and M is chosen to fit the present-time dark energy density. This potential has a tracking behavior, so the wide range of initial conditions eventually converge to one common tracking solution [88]. The tracking solution of the Ratra-Peebles potential gives the slow roll of the ϕ field, i.e. the kinetic energy of ϕ is much less than $V(\phi)$. This is essential for the quintessence to be the dark energy (See the reviews [89, 90]); likewise, the gauged quintessence model requires the slow roll of ϕ field.

The dynamics may alter when the quantum effects are considered [91, 92]. The 1-loop corrected potential of ϕ is given as³ [76]

$$V = V_0 + \frac{\alpha(\alpha+1)\Lambda^2}{32\pi^2} \frac{M^{\alpha+4}}{\phi^{\alpha+2}} + \frac{(V_0'')^2}{64\pi^2} \left(\ln \frac{V_0''}{\Lambda^2} - \frac{3}{2} \right) + \frac{3(m_X^2|_0)^2}{64\pi^2} \left(\ln \frac{m_X^2|_0}{\Lambda^2} - \frac{5}{6} \right), \quad (2.5)$$

where Λ is the cutoff scale, which we will take as the Planck mass ($M_{\text{Pl}} \approx 1.22 \times 10^{19}$ GeV), and $'$ denotes the partial derivative with respect to the ϕ . Then the effective potential of ϕ is $V_{\text{eff}} = V + V_{\text{gauge}}$. Following the discussions in Ref. [76], we find the third term is negligibly small, and the last term gives an upper bound on m_X as $m_X \lesssim 10^{-11}$ GeV.

One important feature of the gauged quintessence model is the evolution of m_X . (For some other examples of the mass-varying particles, see Refs. [93–100].) The masses of ϕ and X are given by

$$m_\phi^2 = \frac{\partial^2 V_{\text{eff}}}{\partial \phi^2}, \quad m_X^2 = g_X^2 \phi^2, \quad (2.6)$$

and m_X evolves when $m_\phi \gtrsim H$. As we will demonstrate in Sec. 3, the X behaves as a non-relativistic matter when $m_X \gtrsim H$. However, the dark gauge boson cannot be the candidate of sole dark matter since the mass of the X can change many orders of magnitude after the matter-radiation equality. So we assume an additional species that gives the dominant contribution to the dark matter relic density. The X density can be amplified by the mass-increasing effect, and this property will be crucial in the production of X as we will demonstrate in Sec. 4.1.

²The FLRW metric with $g_{\mu\nu} = (-1, a^2, a^2, a^2)$ is used.

³One may view the Ratra-Peebles potential as a quantum effective potential. However, it is unnatural to expect that couplings to the quintessence are tuned exactly to cancel the corrections from the gauge boson loops [92].

3 Dynamics of the gauged quintessence model

There are two distinct contributions to the coherent dark gauge boson after inflation. One is the production from the misalignment, which originates from the homogeneous mode at the beginning of the inflation. The wavelength of this mode is much larger than the current observable scale of the universe, so it remains homogeneous until today. The other contribution is the production from the quantum fluctuation (gravitational production). These fluctuations can be exponentially stretched during inflation, and some of the long wavelength fluctuations could remain homogeneous until today.⁴ We will consider the case that only the misalignment production of the X gauge boson is effective; namely, the other contribution is subdominant.

In this section, we discuss the dynamics of a homogeneous mode of X and ϕ field. From this, one can calculate various quantities such as mass and energy density. In brief, the dynamics of the X field and ϕ field are determined by the hierarchy between the mass of each field and the Hubble parameter. In other words, the dynamics of X or ϕ field changes when $H \sim m_X$ or $H \sim m_\phi$, respectively. To simplify the discussion, we define a_{tr} (a_{nr}) as the scale factor when $H \sim m_\phi$ ($H \sim m_X$). The ϕ field follows the tracking solution after the a_{tr} ; and X boson starts coherent oscillation after the a_{nr} , and it behaves as a non-relativistic matter. Also, we denote a_{ini} , a_{end} , and a_{eq} as the scale factor when inflationary, radiation-dominated, and matter-dominated epoch begins.⁵

3.1 Dynamics of the dark gauge boson

The equation of motion of dark gauge boson is obtained from the action (Eq. (2.2)) as

$$\partial_\mu (\sqrt{-g} X^{\mu\nu}) - \sqrt{-g} m_X^2 X^\nu = 0. \quad (3.1)$$

For the homogeneous mode $X_\mu(t, \vec{x}) = X_\mu(t) = (X_0(t), \vec{X}(t))$, and it gives

$$X_0 = 0, \quad \ddot{\vec{X}} + H\dot{\vec{X}} + m_X^2 \vec{X} = 0. \quad (3.2)$$

We set our coordinate such that $\vec{X} = (0, 0, X)$ without the loss of generality, so the energy density of the homogeneous mode is written as

$$\rho_X = \rho_X^{(k)} + \rho_X^{(v)} \quad \text{where} \quad \rho_X^{(k)} = \frac{1}{2a^2} \dot{X}^2 \quad \text{and} \quad \rho_X^{(v)} = \frac{1}{2a^2} m_X^2 X^2. \quad (3.3)$$

In order to find the evolution of the ρ_X , one needs to solve the equation of motion (Eq. (3.2)). To do so, we use the physical field defined as $\bar{X} = X/a$, and rewrite Eq. (3.2) as

$$\ddot{\bar{X}} + 3H\dot{\bar{X}} + \left(m_X^2 + \frac{1 - 3w_b}{2} H^2 \right) \bar{X} = 0, \quad (3.4)$$

where w_b ⁶ is the background equation of state. This equation is analogous to the equation of motion for the scalar field, except for the Hubble-induced mass term.

⁴A more detailed discrimination of the two, see, e.g., Ref. [101].

⁵We assumed instant reheating to simplify discussions. Therefore, a_{end} corresponds to both the end of inflation and the beginning of the radiation-dominated epoch.

⁶ $w_b = -1$ in the inflationary era, $w_b = 1/3$ in the radiation dominated era, and $w_b = 0$ in the matter dominated era.

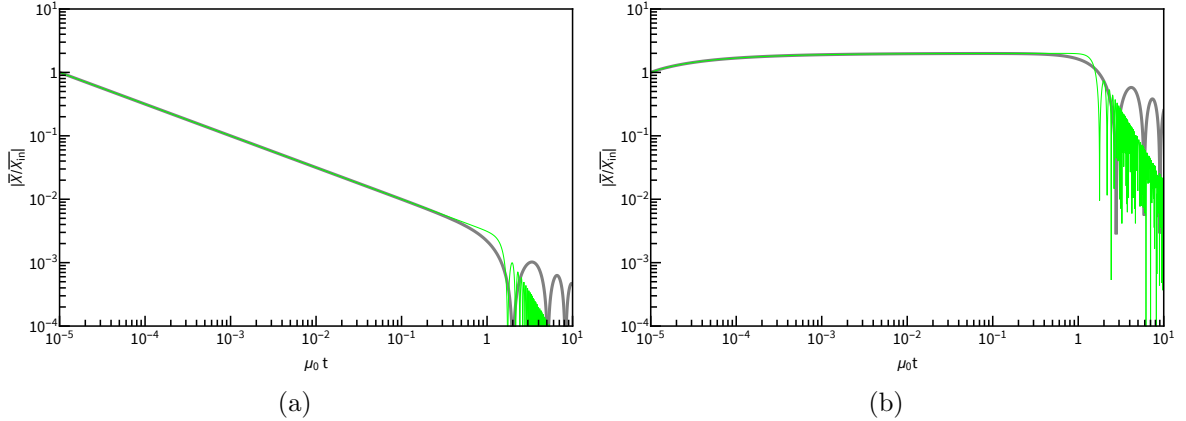


Figure 1: Evolution of the dark gauge boson field normalized by the initial field value \overline{X}_{in} during the radiation-dominated era. The gray curve has a constant mass $m_X = \mu_0$, and the green curve has time varying mass $m_X = \mu_0(\mu_0 t)^3$. The numerical evaluation starts at $\mu_0 t = 10^{-5}$. (a) For the potential energy-dominated case, $\overline{X} \propto 1/\sqrt{t} \propto 1/a$. (b) For the kinetic energy-dominated case, \overline{X} is almost constant, except for the $\mathcal{O}(1)$ modification. For both cases, the evolution of the \overline{X} until $H \sim m_X$ is not affected by the m_X . The bottoms of oscillations reach 0, although they do not appear due to the resolution of the plots.

The solution of this equation when $m_X \ll H$ is [85]

$$\overline{X} = c_1 a^{-1} + c_2 a^{(3w_b-1)/2} \quad \Leftrightarrow \quad X = c_1 + c_2 a^{(3w_b+1)/2}, \quad (3.5)$$

where the c_1 and c_2 are undetermined coefficients, which can be determined by the initial condition. The c_1 solution corresponds to the potential energy dominated initial condition ($\rho_X^{(k)} \ll \rho_X^{(v)}$), and c_2 solution corresponds to the kinetic energy dominated initial condition ($\rho_X^{(k)} \gg \rho_X^{(v)}$). These solutions are valid even when $w_b = 1/3$. We give some numerical examples of \overline{X} evolution during the radiation-dominated era in Fig. 1. Then the evolution of the X density when $m_X \ll H$ is given as

$$\begin{cases} \rho_X = \frac{1}{2} \left(\left(\frac{3w_b+1}{2} \right)^2 H^2 + m_X^2 \right) \overline{X}^2 \propto a^{-4} & \text{for } \rho_X^{(k)} \gg \rho_X^{(v)}, \\ \rho_X = \frac{1}{2} m_X^2 \overline{X}^2 \propto m_X^2 a^{-2} & \text{for } \rho_X^{(k)} \ll \rho_X^{(v)}. \end{cases} \quad (3.6)$$

We wrote $m_X^2 a^{-2}$ instead of a^{-2} to explicitly show the mass varying effect.

On the other hand, the evolution of X when $m_X \gtrsim H$ is found in the adiabatic limit as [102–104]

$$\overline{X} \propto \text{Re} \left[\frac{1}{\sqrt{a^3 m_X}} e^{i \int dt m_X} \right] \quad \Leftrightarrow \quad X \propto \text{Re} \left[\frac{1}{\sqrt{a m_X}} e^{i \int dt m_X} \right], \quad (3.7)$$

where the $\text{Re}[f]$ denotes the real part of f . Hence, the kinetic energy and potential energy of the X averaged over the oscillations are the same in this regime. Thus the energy density evolves as

$$\rho_X \propto m_X a^{-3}, \quad (3.8)$$

Initial condition	$H \gg m_X$	$H \lesssim m_X$
$\rho_X^{(k)} \gg \rho_X^{(v)}$	$\rho_X \propto a^{-4}$	$\rho_X \propto m_X a^{-3}$
$\rho_X^{(k)} \ll \rho_X^{(v)}$	$\rho_X \propto m_X^2 a^{-2}$	$\rho_X \propto m_X a^{-3}$

Table 1: Evolution of ρ_X for different initial conditions. For both cases, the energy density evolves as a non-relativistic species after $H \sim m_X$.

which is the same as the evolution of the non-relativistic particle. We summarize the results in Tab. 1.

Interestingly, the energy density of the dark gauge boson can be largely enhanced if the mass of X increases during cosmic evolution. Also, this effect is much more noticeable for the potential energy-dominated initial condition. Thus, the dark gauge boson energy density could even be comparable to the CDM energy density despite the exponential suppression during inflation.

Although there is a mass-varying effect, it is hard to achieve a sufficient relic density of X in the kinetic energy-dominated scenario due to a^{-4} suppression. Assuming that X becomes non-relativistic after inflation, the present energy density of X is at most 10^{-50} times that of matter. There is a possibility that X becomes non-relativistic during inflation but the kinetic energy-dominated case cannot provide sufficient energy in this case, too. Therefore, we will consider the potential energy-dominated case only, hereafter.

3.2 Dynamics of the quintessence

The equation of motion for the homogeneous mode of ϕ is given as

$$\ddot{\phi} + 3H\dot{\phi} + \frac{\partial V_{\text{eff}}}{\partial \phi} = 0. \quad (3.9)$$

The dominant terms of V_{eff} are⁷

$$V_{\text{eff}} \approx \frac{\alpha(\alpha+1)\Lambda^2}{32\pi^2} \frac{M^{\alpha+4}}{\phi^{\alpha+2}} + \frac{1}{2a^2} g_X^2 X^2 \phi^2. \quad (3.10)$$

So, the dynamical minimum of the potential is generated from the combination of the inverse power term and a quadratic term. The ϕ field and mass of ϕ at the minimum of V_{eff} are given as

$$\begin{aligned} \phi_{\text{min}} &= \left(\frac{\alpha(\alpha+1)(\alpha+2)\Lambda^2 M^{\alpha+4}}{32\pi^2 g_X^2 \bar{X}^2} \right)^{1/(\alpha+4)} \propto \bar{X}^{-2/(\alpha+4)}, \\ m_\phi(\phi_{\text{min}}) &= \sqrt{\alpha+4} g_X \bar{X} \propto \bar{X}. \end{aligned} \quad (3.11)$$

The dynamics of quintessence is determined by the relative size of m_ϕ and H , and the magnitude of V_{gauge}'' . If $H \gg m_\phi$, ϕ becomes constant due to the Hubble friction, and so the m_ϕ is fixed, too. On the other hand, if $H \lesssim m_\phi$, then the ϕ field rolls down the potential. Two

⁷The tree-level potential V_0 dominates only when $\phi > \sqrt{\alpha(\alpha+1)\Lambda^2/(32\pi^2)} \sim 0.1\Lambda$. If we take $\Lambda = M_{\text{Pl}}$, the first term in Eq. (3.10) mostly governs the dynamics over the tree-level potential except for a short period near present [76].

different situations can happen in this case. If the $V''_{\text{gauge}} \gtrsim H^2$, the potential is sufficiently steep about the minimum so the ϕ field follows the minimum of the potential. Thus, we approximate that $\phi \sim \phi_{\text{min}}$. However, if $V''_{\text{gauge}} \ll H^2$, ϕ field cannot reach the potential minimum during the Hubble time, and V_{gauge} can be ignored. In this case, the ϕ field rolls down until $m_\phi \sim H$, and follows the tracking solution of the inverse power potential. During the tracking, the scaling of ϕ and m_ϕ becomes [51]

$$\phi \propto a^{\frac{3(w_b+1)}{\alpha+4}}, \quad m_\phi \propto a^{-\frac{3(w_b+1)}{2}}. \quad (3.12)$$

Hence, the scaling behavior of m_ϕ is the same as the H , and the $\phi \sim \text{constant}$ during inflation.

Let us discuss a viable scenario to produce sufficient relic X density. We consider that m_ϕ is much larger than H_{inf} at the beginning of inflation but eventually becomes comparable to H_{inf} before inflation was terminated⁸. Therefore, the ϕ field initially moves along the potential minimum and joins the tracking solution before the a_{end} . Schematic description of m_ϕ , m_X , and H of this scenario is given in Fig. 2. Using the dynamics of \bar{X} and ϕ discussed in the earlier part of this section, one can obtain the scaling behavior of ρ_X and ρ_ϕ . The dynamics of \bar{X} , ϕ (m_X), ρ_X and ρ_ϕ are summarized in the following texts and Tab. 2. For simplicity, we take that the V_{gauge} is negligible after a_{tr} . Also, we omit the short dark energy or tree-level potential dominated epoch right before the a_0 . This simplification does not alter the order of magnitude estimation of the relic densities of X , and ϕ .

	\bar{X}	ϕ	ρ_X	ρ_ϕ
$a_{\text{ini}} < a < a_{\text{tr}}$	$\propto a^{-1}$	$\propto a^{\frac{2}{\alpha+4}}$	$\propto a^{-\frac{2\alpha+4}{\alpha+4}}$	$\propto a^{-\frac{2\alpha+4}{\alpha+4}}$
$a_{\text{tr}} < a < a_{\text{end}}$	$\propto a^{-1}$	$\sim \text{constant}$	$\propto a^{-2}$	$\sim \text{constant}$
$a_{\text{end}} < a < a_{\text{nr}}$	$\propto a^{-1}$	$\propto a^{\frac{4}{\alpha+4}}$	$\propto a^{-\frac{2\alpha}{\alpha+4}}$	$\propto a^{-\frac{4\alpha+8}{\alpha+4}}$
$a_{\text{nr}} < a < a_{\text{eq}}$	$\propto a^{-\frac{3\alpha+16}{2\alpha+8}}$	$\propto a^{\frac{4}{\alpha+4}}$	$\propto a^{-\frac{3\alpha+8}{\alpha+4}}$	$\propto a^{-\frac{4\alpha+8}{\alpha+4}}$
$a_{\text{eq}} < a < a_0$	$\propto a^{-\frac{3\alpha+15}{2\alpha+8}}$	$\propto a^{\frac{3}{\alpha+4}}$	$\propto a^{-\frac{3\alpha+9}{\alpha+4}}$	$\propto a^{-\frac{3\alpha+6}{\alpha+4}}$

Table 2: Behaviors of \bar{X} , ϕ , ρ_X and ρ_ϕ when $m_\phi > H_{\text{inf}}$ at the beginning of inflation and $m_\phi \sim H_{\text{inf}}$ is achieved during inflation.

Since we have determined the scaling behaviors, we can calculate various quantities if we know the a_{ini} , a_{tr} , a_{end} , a_{nr} . For simplicity, we assume the instant reheating⁹, so the a_{end} is given from the following relation as

$$H_{\text{inf}} \sim \sqrt{\Omega_r} H_0 \left(\frac{a_0}{a_{\text{end}}} \right)^2. \quad (3.13)$$

⁸Although the scenarios such that $m_\phi \ll H_{\text{inf}}$ or $m_\phi \gg H_{\text{inf}}$ during the entire inflation era are possible, they cannot provide sufficient relic density of X . Therefore, we will not deal with these scenarios in the main text. Refer to Appendix A.

⁹Under the assumption of the instant reheating, we may estimate the reheating temperature T_{rh} via $\rho_{\text{inf}} = \rho_{\text{rad}}$ where $\rho_{\text{rad}} = (g_*(T_{\text{rh}})\pi^2/30)T_{\text{rh}}^4/m_{\text{Pl}}^2$ with $g_*(T)$ the effective number of relativistic degrees of freedom at T , and $m_{\text{Pl}} = M_{\text{Pl}}/\sqrt{8\pi}$.

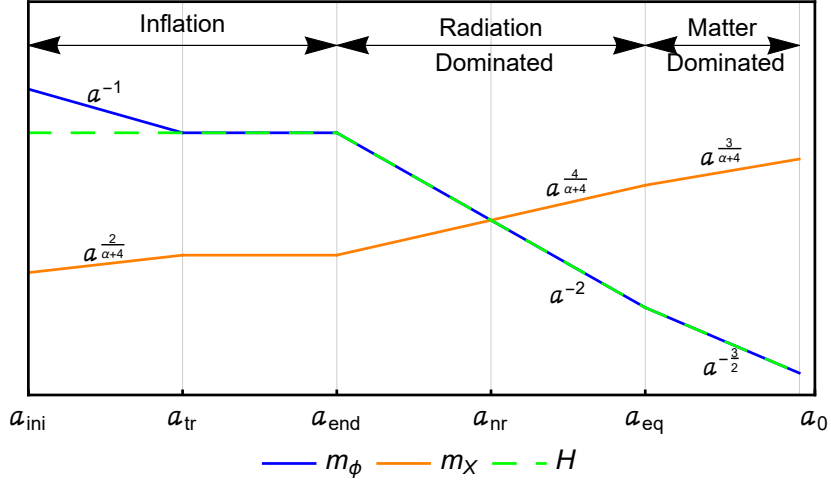


Figure 2: Schematic description of scaling behavior of m_ϕ , m_X and H for the scenario in Sec. 3.2. Tracking behavior begins at a_{tr} when $m_\phi \sim H$ is achieved. In this scenario, it is assumed that a_{tr} is in the inflationary era. a_{nr} , when $m_X \sim H$ is in the radiation dominated era. This figure is a rough description and the relative scales are not exact. The blank region before the a_0 corresponds to the dark energy dominated era with the tree-level potential domination. This era is extremely short compared to other eras.

Also, we take the number of e-folds of inflation as $N = 60$. This gives $a_{\text{ini}} = e^{-60} a_{\text{end}}$. Let us determine the a_{tr} and a_{nr} . The Eqs. (3.6) and (3.11) gives

$$m_\phi \sim \frac{\sqrt{2(\alpha+4)\rho_X}}{\phi} \sim \sqrt{2(\alpha+4)\rho_X}^{\frac{\alpha+4}{2\alpha+4}} \left(\frac{\alpha(\alpha+1)(\alpha+2)\Lambda^2 M^{\alpha+4}}{64\pi^2} \right)^{-\frac{1}{\alpha+2}} \quad \text{for } a \lesssim a_{\text{tr}}. \quad (3.14)$$

Using that $m_\phi \propto a^{-1}$ for $a < a_{\text{tr}}$, and $m_\phi \sim H$ at a_{tr} ,

$$\frac{a_{\text{tr}}}{a_{\text{ini}}} \sim \sqrt{2(\alpha+4)\rho_X}^{\frac{\alpha+4}{2\alpha+4}} \left(\frac{\alpha(\alpha+1)(\alpha+2)\Lambda^2 M^{\alpha+4}}{64\pi^2} \right)^{-\frac{1}{\alpha+2}} H_{\text{inf}}^{-1}. \quad (3.15)$$

Also, ϕ at a_{tr} is given as

$$\phi(a_{\text{tr}}) \sim \left(\frac{\alpha(\alpha+1)(\alpha+2)(\alpha+4)\Lambda^2 M^{\alpha+4}}{32\pi^2 H_{\text{inf}}^2} \right)^{\frac{1}{\alpha+4}}. \quad (3.16)$$

The value of ϕ remains constant during the remaining inflationary era. During the radiation domination era, $\phi \propto a^{\frac{4}{\alpha+4}}$, and $H \propto a^{-2}$. Since $H \sim m_X$ at a_{nr} , we have

$$m_X(a_{\text{nr}}) \sim g_X \phi(a_{\text{tr}}) \left(\frac{a_{\text{nr}}}{a_{\text{end}}} \right)^{\frac{4}{\alpha+4}} \sim H_{\text{inf}} \left(\frac{a_{\text{nr}}}{a_{\text{end}}} \right)^{-2}. \quad (3.17)$$

This relation gives $a_{\text{nr}}/a_{\text{end}}$ as

$$\frac{a_{\text{nr}}}{a_{\text{end}}} \sim g_X^{-\frac{\alpha+4}{2\alpha+12}} H_{\text{inf}}^{\frac{1}{2}} \left(\frac{\alpha(\alpha+1)(\alpha+2)(\alpha+4)\Lambda^2 M^{\alpha+4}}{32\pi^2} \right)^{-\frac{1}{2\alpha+12}}. \quad (3.18)$$

Therefore, we can determine all relevant scale factors required to calculate various quantities for this scenario.

4 Constraints

In this section, we show various constraints on the scenario in the previous section, especially for $\alpha = 1$. We set $M = 2.2 \times 10^{-6}$ GeV to reproduce the present dark energy density.

4.1 Backreaction of ρ_X during the inflation

In order to have a successful inflation, the energy density of X should be much smaller than the inflaton energy density. Since the energy density of X monotonically decreases during inflation, the energy density of X at the start of inflation has an upper limit by

$$\rho_X(a_{\text{ini}}) \ll \rho_{\text{inf}} = 3m_{\text{Pl}}^2 H_{\text{inf}}^2, \quad (4.1)$$

where $m_{\text{Pl}} = M_{\text{Pl}}/\sqrt{8\pi} \simeq 2.4 \times 10^{18}$ GeV is the reduced Planck mass. Here, the ρ_{inf} is the energy density of inflaton. If we assume that the ϕ settles down close to the potential minimum, we have $\rho_\phi \sim \rho_X$. So the backreaction from the ϕ can be also verified by Eq. (4.1).

The quantitative constraint on the main scenario is the following. Using Tab. 2, we have

$$\rho_X(a_{\text{ini}}) = \rho_X(a_0) \left(\frac{a_{\text{eq}}}{a_0}\right)^{-12/5} \left(\frac{a_{\text{nr}}}{a_{\text{eq}}}\right)^{-11/5} \left(\frac{a_{\text{end}}}{a_{\text{nr}}}\right)^{-2/5} \left(\frac{a_{\text{tr}}}{a_{\text{end}}}\right)^{-2} \left(\frac{a_{\text{ini}}}{a_{\text{tr}}}\right)^{-6/5}, \quad (4.2)$$

where a_{tr} and a_{nr} can be calculated from Eqs. (3.15) and (3.18). When we assume $\ln(a_{\text{end}}/a_{\text{ini}}) = 60$, for example, the constraint on $\rho_X(a_{\text{ini}})$ to avoid the backreaction is written as

$$\frac{\rho_X(a_{\text{ini}})}{3m_{\text{Pl}}^2 H_{\text{inf}}^2} = 3.5 \times 10^{-17} \left(\frac{\rho_X(a_0)}{\rho_{\text{CDM}}(a_0)}\right)^{3/5} \left(\frac{H_{\text{inf}}}{10 \text{ GeV}}\right)^{-7/5} \left(\frac{g_X}{10^{-31}}\right)^{27/70} < 1. \quad (4.3)$$

For a fixed amount of ρ_X , we have a lower bound on H_{inf} or an upper bound on g_X .

4.2 Isocurvature fluctuation

The fluctuation of the X field is an independent degree of freedom from the inflaton fluctuation. Therefore, the isocurvature fluctuation is generated from the quantum fluctuation of the X . Since the production of the transverse modes is suppressed for the minimal vector field [83], only the longitudinal modes contribute to the fluctuation of the X . The power spectrum of the longitudinal mode is defined as

$$\langle \bar{X}_L(\vec{k}_1) \bar{X}_L^*(\vec{k}_2) \rangle \equiv \frac{2\pi^2}{k^3} \mathcal{P}_{\bar{X}_L}(\vec{k}_1) (2\pi)^3 \delta^{(3)}(\vec{k}_1 - \vec{k}_2), \quad (4.4)$$

and one can calculate that (see App. B for the detail)

$$\mathcal{P}_{\bar{X}_L}(\vec{k}, a_{\text{end}}) = \zeta \left(\frac{k H_{\text{inf}}}{2\pi a_{\text{end}} m_X(a_{\text{end}})} \right)^2, \quad \zeta = \begin{cases} 1 & \text{for } a_{\text{tr}} < \frac{k}{H_{\text{inf}}}, \\ \frac{2^{14/5}}{\pi} \Gamma^2\left(\frac{19}{10}\right) \left(\frac{a_{\text{tr}} H_{\text{inf}}}{k}\right)^{4/5} & \text{for } a_{\text{tr}} > \frac{k}{H_{\text{inf}}}. \end{cases} \quad (4.5)$$

Here, the power spectrum is proportional to the inverse of m_X , so the isocurvature constraint is stronger for the smaller m_X .

Then, the isocurvature fluctuation is given by¹⁰ [105–107]

$$\begin{aligned}
S_{\text{CDM}}(\vec{k}, a_{\text{lss}}) &\sim \frac{\delta\rho_X(\vec{k}, a_{\text{lss}})}{\rho_X(a_{\text{lss}}) + \rho_{\text{CDM}}(a_{\text{lss}})} \sim \frac{2m_X^2(a_{\text{lss}})\bar{X}(a_{\text{lss}})\delta\bar{X}(k, a_{\text{lss}})}{m_X^2(a_{\text{lss}})\bar{X}^2(a_{\text{lss}}) + 2\rho_{\text{CDM}}(a_{\text{lss}})} \\
&\sim \frac{2\sqrt{\mathcal{P}_{\bar{X}_L}(\vec{k}, a_{\text{end}})/\bar{X}(a_{\text{end}})}}{1 + \rho_{\text{CDM}}(a_{\text{lss}})/\rho_X(a_{\text{lss}})},
\end{aligned} \tag{4.6}$$

where the $\delta\rho_X$ is evaluated at the uniform density slicing [108], and the a_{lss} is the scale factor at last scattering surface. In the last step, we used that the evolution of the super horizon mode and the zero modes are the same after the inflation. (See, App. B.)

The $\bar{X}(a_{\text{end}})$ can be calculated as¹¹

$$\bar{X}(a_{\text{end}}) \sim 5.4 \times 10^{21} \text{ GeV} \left(\frac{\rho_X(a_0)}{\rho_{\text{CDM}}} \right)^{1/2} \left(\frac{H_{\text{inf}}}{10 \text{ GeV}} \right)^{1/2} \left(\frac{g_X}{10^{-31}} \right)^{-19/28}. \tag{4.7}$$

Also, from the conservation of the number density of the dark gauge boson, i.e. $\rho_X^0/m_X^0 = a^3\rho_X/m_X$, we have

$$\frac{\rho_{\text{CDM}}(a_{\text{lss}})}{\rho_X(a_{\text{lss}})} \sim 67 \frac{\rho_{\text{CDM}}(a_0)}{\rho_X(a_0)}. \tag{4.8}$$

Then, the isocurvature constraint can be calculated from the $S_{\text{CDM}} \lesssim 9 \times 10^{-6}$ at $k \sim 0.05 \text{ Mpc}^{-1}$ [109]¹². We show this constraint in figure. 3.

4.3 Stochastic correction to the quintessence evolution

So far, we assumed that the homogeneous mode of the ϕ field follows the trajectory determined by the equation of motion (Eq. (3.9)). Actually, this is not always true since the quantum fluctuations of the quintessence field can affect the motion of the quintessence field [110, 111]. During the inflation, fluctuations of ϕ field can exit the horizon (i.e. $k/a < H_{\text{inf}}$), and gives a random jump on the homogeneous part of the ϕ field [110]. Therefore, the evolution of the homogeneous part of the ϕ field is under a stochastic process [112, 113]. However, we will demonstrate that the stochastic effect is negligible for the scenario in Sec. 3.

Let us split the quintessence field into the homogeneous part¹³ (ϕ_0) and inhomogeneous perturbation ($\delta\phi$) such that $\phi = \phi_0 + \delta\phi$. The evolution of the Fourier component with momentum k is described by the Klein-Gordon equation [110] as

$$\ddot{\tilde{\phi}}_k(t) + 3H\dot{\tilde{\phi}}_k(t) + ((k/a)^2 + m_\phi^2)\tilde{\phi}_k(t) = 0, \tag{4.9}$$

where the $\tilde{\phi}_k(t)$ is the fluctuation with a wave number k . For the nearly massless case, the power spectrum of the fluctuation is given by $P_\phi(k, t) \approx (H/(2\pi))^2$. This implies that the

¹⁰We assume that the dark gauge boson constitutes a fraction of total cold dark matter, and denote the other CDM component as ρ_{CDM} . If the ρ_X is comparable to the ρ_{CDM} , the CMB fitting parameters may change. But, we will assume that this does not significantly affect the order of magnitude constraints given in this section.

¹¹This implies that the X/a may have a super Planckian value for $a \ll a_{\text{nr}}$. We will accept this possibility and suppose that UV physics above the Planck scale does not significantly affect the following discussion.

¹²The CMB power spectrum probes $k = 0.002 - 0.1 \text{ Mpc}^{-1}$. In the mass unit, this corresponds to $k = 10^{-41} - 7 \times 10^{-40} \text{ GeV}$.

¹³Formally, the homogeneous part is a collection of long wavelength mode with $k < aH$ [113].

size of the random jump of the ϕ field per Hubble time is about $H/(2\pi)$ [110]. On the other hand, compared to the nearly massless case, a magnitude of fluctuation is suppressed when $m_\phi \gtrsim H$.

In the scenario in Sec. 3, the ϕ field is initially trapped in the potential minimum with m_ϕ larger than H . Thus, we can approximate that the ϕ follows the potential minimum, and the stochastic effect is negligible. After the a_{tr} , the V_{gauge} becomes too shallow, so the ϕ field does not follow the potential minimum anymore but enters the slow roll tracking regime. So the random motion of the ϕ field is accumulated about $\phi(a_{\text{tr}})$. If the motion of the ϕ driven by the potential is dominant over the stochastic effect, we can approximate that the trajectory of the ϕ field is solely given by the equation of motion.

Therefore, it is required that the standard deviation from the random jump is less than the ϕ_0 , and we have the following condition as

$$\phi_0 \sim \phi(a_{\text{tr}}) \sim \left(\frac{15\Lambda^2 M^5}{16\pi^2 H_{\text{inf}}^2} \right)^{1/5} > \frac{H_{\text{inf}}}{2\pi} \sqrt{\Delta N}, \quad (4.10)$$

where the ΔN is the number of e-folding between the a_{tr} and a_{end} . If we choose $\Delta N = 60$ as a conservative manner, then the upper bound on H_{inf} is given as

$$H_{\text{inf}} \lesssim 16 \text{ GeV}. \quad (4.11)$$

Figure 3 summarizes various constraints discussed in this section and also shows other constraints from the literature. The orange region shows the constraint from the backreaction of the X boson to inflation. Since the inflaton energy density is proportional to H_{inf} , this gives the lower bound on H_{inf} . On the other hand, the isocurvature fluctuation of X boson and stochastic motion of the ϕ field is proportional to H_{inf} , so they give the upper bound on H_{inf} as blue and light blue constraints. The gray region is excluded from the quantum correction of the X boson to the ϕ potential [76]. This constraint is necessary to protect the slow roll of the ϕ field. However, this might be alleviated, if some unknown mechanism can cancel the gauge boson loop diagrams or one takes the Ratra-Peebles potential as a quantum effective potential which already includes all the quantum corrections. The red region on the left is the constraint from the Lyman- α forest. If the mass of dark matter is extremely small, the wave nature of dark matter can suppress the growth of the power spectrum below its de Broglie wavelength. (See Ref. [116] for a review.) This gives a lower bound for the dark matter component in $10^{-31} - 10^{-29}$ GeV range. The ultra light boson of mass range roughly $10^{-30} - 10^{-20}$ GeV may source the black hole superradiance [117–123], which corresponds to the left half of the parameter region in the plot. The weak gravity conjecture states that a too small gauge coupling may not be congruous with the quantum gravity [124]. This leads to the following condition on the inflationary scenario as [125, 126]

$$H_{\text{inf}} \lesssim g_X^{1/3} M_{\text{Pl}}. \quad (4.12)$$

The yellow area shows the disfavored region from the weak gravity conjecture.

We want to remind you that we do not expect the X boson as a whole dark matter. The back reaction (orange), isocurvature (blue), and Lyman- α (light red) constraints become weaker if the X boson constitutes only a fraction of a whole dark matter. In this sense, the constraints are conservative bounds for this scenario.

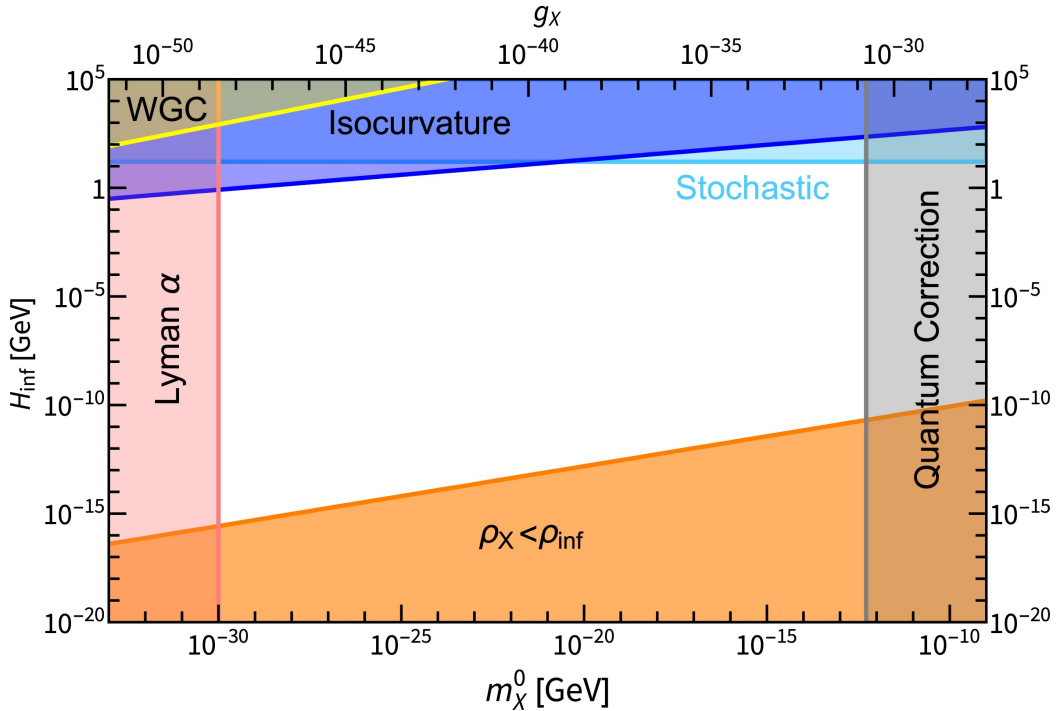


Figure 3: Constraints on the scenario with $\alpha = 1$ when $\rho_X(a_0)$ is the expected dark matter density. The blue region is excluded by the isocurvature fluctuation constraint. The red region is excluded by the $\rho_X < \rho_{\text{inf}}$ (Back reaction of the ρ_X) during the inflation. The light blue region is constrained by the stochastic correction to the ϕ field. The gray region is disfavored by the quantum correction in the gauged quintessence potential [76]. The light red region is excluded by the Lyman- α forest [114, 115]. The yellow area is disfavored by the weak gravity conjecture. The present ϕ value is $\phi_0 \approx 3 \times 10^{18}$ GeV.

5 Summary and discussion

In this paper, we investigated the misalignment mechanism for a vector boson that couples to the quintessence dark energy field. Because of the scale factor suppression of the vector boson energy density, the naive misalignment mechanism does not produce a sizable amount of the coherent vector boson. In the gauged quintessence model, the mass of the dark gauge boson is proportional to the quintessence field value. Thus, it can increase many orders of magnitude during cosmic evolution. So even if the energy density of the dark gauge boson gets exponential suppression from inflation, it is possible to produce a large fraction of the relic dark gauge boson energy density. We showed that the relic density of the dark gauge boson could be comparable to the known CDM relic density because of the mass-increasing effect. The high-dimensional operators are assumed to be zero, though, as they should be suppressed to preserve the X field dynamics in the early universe.

There are various scenarios of the misalignment mechanism for the vector boson production, which have additional ingredients such as kinetic coupling to the inflaton [85, 87, 127] or non-minimal coupling to gravity [84, 86], where such new ingredients were primarily introduced for the sizable production of vector boson energy density. However, in the gauged quintessence model, the coupling between the vector boson and quintessence dark energy

field was not introduced to explain the production of vector boson. Such a coupling naturally arises when we impose a gauge symmetry to the dark energy sector. In that sense, the gauged quintessence model can provide a rather natural misalignment production scenario for the vector boson.

Even though our analysis is based on a specific potential, the message that the mass-increasing effect of vector bosons can mitigate strong suppression of the vector boson energy density during inflation holds generically.

Acknowledgments

This work was supported in part by the JSPS KAKENHI (Grant No. 19H01899) and the National Research Foundation of Korea (Grant No. NRF-2021R1A2C2009718).

A Extra scenarios

In this appendix, We discuss extra scenarios which were not shown in Sec. 3.2. As it was discussed, the dynamics of quintessence are determined by the relative size of m_ϕ , $\sqrt{V''_{\text{gauge}}}$, and H . In the main text, we have $m_\phi \gg H$ at the beginning of inflation, and $m_\phi \sim H$ is achieved during inflation. However, other scenarios are possible such that the relations $m_\phi \gg H$ or $m_\phi \ll H$ might be maintained during the entire inflationary era¹⁴. We describe the behaviors of m_X and m_ϕ for each scenario in Fig. 4, and corresponding dynamics are summarized in the following texts and tables. As we discussed in Sec. 4, we ignore the short dark energy dominated era with the tree-level potential domination.

- Extra scenario (i): $m_\phi \gg H_{\text{inf}}$ during the entire inflation era.

	\bar{X}	ϕ	ρ_X	ρ_ϕ
$a_{\text{ini}} < a < a_{\text{end}}$	$\propto a^{-1}$	$\propto a^{\frac{2}{\alpha+4}}$	$\propto a^{-\frac{2\alpha+4}{\alpha+4}}$	$\propto a^{-\frac{2\alpha+4}{\alpha+4}}$
$a_{\text{end}} < a < a_{\text{nr}}$	$\propto a^{-1}$	$\propto a^{\frac{2}{\alpha+4}}$	$\propto a^{-\frac{2\alpha+4}{\alpha+4}}$	$\propto a^{-\frac{2\alpha+4}{\alpha+4}}$
$a_{\text{nr}} < a < a_{\text{eq}}$	$\propto a^{-\frac{3(\alpha+4)}{2(\alpha+3)}}$	$\propto a^{\frac{3}{\alpha+3}}$	$\propto a^{-\frac{3\alpha+6}{\alpha+3}}$	$\propto a^{-\frac{3\alpha+6}{\alpha+3}}$
$a_{\text{eq}} < a < a_0$	$\propto a^{-\frac{3(\alpha+4)}{2(\alpha+3)}}$	$\propto a^{\frac{3}{\alpha+3}}$	$\propto a^{-\frac{3\alpha+6}{\alpha+3}}$	$\propto a^{-\frac{3\alpha+6}{\alpha+3}}$

Table 3: Dynamics for the extra scenario (i).

In this scenario, the initial V_{gauge} is the largest of all three scenarios. Therefore, it takes a long time for m_ϕ to be comparable to H . Since the ϕ field follows minimum of the potential before a_{tr} , the scaling of the m_ϕ is given as $m_\phi \propto a^k$ with $k \geq -2$. This means that m_ϕ is always larger than H even during the radiation-dominated epoch, so we get $a_{\text{tr}} > a_{\text{eq}}$. To obtain the accelerated expansion, a_{tr} should be smaller than a_0 ; since the slow roll of ϕ cannot be achieved if the ϕ field runs along the potential minimum. However, an explicit calculation shows that $a_{\text{tr}} > a_0$, so the ϕ cannot be the dark energy.

- Extra Scenario (ii): $m_\phi \ll H_{\text{inf}}$ during the entire inflation era.

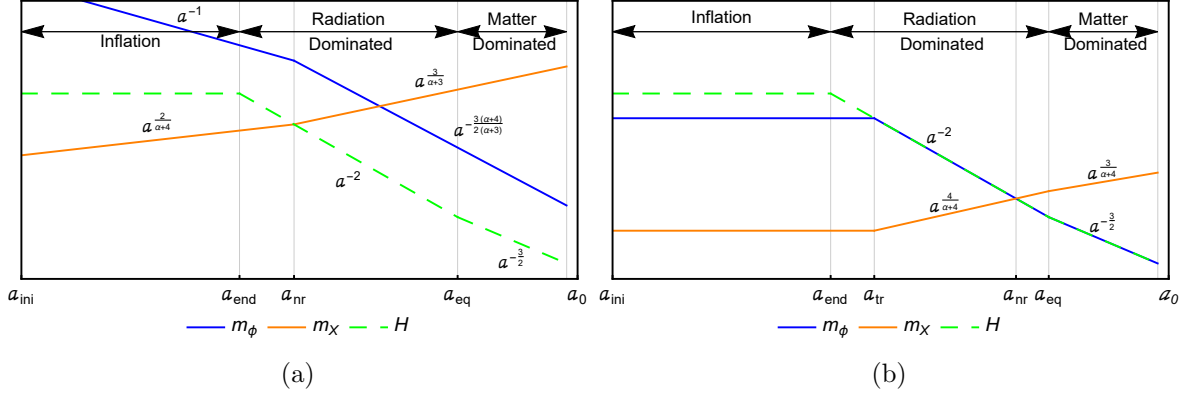


Figure 4: Schematic description of scaling behavior of m_ϕ , m_X and H for the extra scenarios in App. A. (a) $m_\phi \gg H$ during the entire inflationary era. (b) $m_\phi \ll H$ during the entire inflationary era. Refer to figure 2 for the explanation of the blank regime at the right of each figure.

	\bar{X}	$\phi \propto m_X$	ρ_X	ρ_ϕ
$a_{\text{ini}} < a < a_{\text{end}}$	$\propto a^{-1}$	$\sim \text{constant}$	$\propto a^{-2}$	$\sim \text{constant}$
$a_{\text{end}} < a < a_{\text{tr}}$	$\propto a^{-1}$	$\sim \text{constant}$	$\propto a^{-2}$	$\sim \text{constant}$
$a_{\text{tr}} < a < a_{\text{nr}}$	$\propto a^{-1}$	$\propto a^{\frac{4}{\alpha+4}}$	$\propto a^{-\frac{2\alpha}{\alpha+4}}$	$\propto a^{-\frac{4\alpha+8}{\alpha+4}}$
$a_{\text{nr}} < a < a_{\text{eq}}$	$\propto a^{-\frac{3\alpha+16}{2\alpha+8}}$	$\propto a^{\frac{4}{\alpha+4}}$	$\propto a^{-\frac{3\alpha+8}{\alpha+4}}$	$\propto a^{-\frac{4\alpha+8}{\alpha+4}}$
$a_{\text{eq}} < a < a_0$	$\propto a^{-\frac{3\alpha+15}{2\alpha+8}}$	$\propto a^{\frac{3}{\alpha+4}}$	$\propto a^{-\frac{3\alpha+9}{\alpha+4}}$	$\propto a^{-\frac{3\alpha+6}{\alpha+4}}$

Table 4: Dynamics for the extra scenario (ii).

For the second extra scenario, both m_X and m_ϕ are smaller than H_{inf} during inflation. For this scenario to work, H_{inf} should be large and g_X should be very small. However, this scenario could not provide sufficient density of $\rho_X(a_0)$. To have a sensible scenario for $\alpha = 1$, g_X should be smaller than 10^{-61} and it is disfavored by Lyman- α spectrum or weak gravity conjecture.

B Growth of the fluctuations

In this appendix, we discuss the evolution of the longitudinal mode, especially for the scenario in Sec. 3. The Fourier component of the X field is written as

$$\mathbf{X}_\mu(\vec{k}, \tau) = \int d^3x X_\mu(x) e^{-i\vec{k}\cdot\vec{x}}, \quad (\text{B.1})$$

where τ is the conformal time defined by $d\tau = dt/a$. Then, the longitudinal part of the X boson is obtained from the following decomposition, $\vec{X} = \vec{X}_T + \hat{k}X_L$ with $\hat{k} \equiv \vec{k}/|\vec{k}|$, and $\vec{k} \cdot \vec{X}_T = 0$.

¹⁴If $m_\phi \ll H$, then ϕ is frozen by Hubble friction. Since H is constant during inflation, $m_\phi \ll H$ is maintained in the entire inflationary era, once this relationship is initially achieved.

Hence, the action for the longitudinal mode is written as

$$S_L = \frac{1}{2} \int \frac{d\tau d^3k}{(2\pi)^3} \left(\frac{a^2 m_X^2}{k^2 + a^2 m_X^2} |\mathbf{X}'_L|^2 - a^2 m_X^2 |\mathbf{X}_L|^2 \right), \quad (\text{B.2})$$

where \prime denotes the derivative with respect to τ unlike the main text. Note that the kinetic term is not canonical. One can obtain the canonically normalized action by using the redefined field $\mathbf{X}_L^c \equiv am_X \mathbf{X}_L / \sqrt{k^2 + a^2 m_X^2} = g \mathbf{X}_L$,

$$S_L = \frac{1}{2} \int \frac{d\tau d^3k}{(2\pi)^3} \left(|\mathbf{X}'_L|^2 - \left(k^2 + a^2 m_X^2 - \frac{g''}{g} \right) |\mathbf{X}_L^c|^2 \right), \quad (\text{B.3})$$

where

$$\frac{g''}{g} = \frac{k^2}{k^2 + a^2 m_X^2} \left(\frac{a''}{a} + \frac{\phi''}{\phi} + \frac{2a'\phi'}{a\phi} - \frac{3a^2 m_X^2}{k^2 + m_X^2} \left(\frac{a'}{a} + \frac{\phi'}{\phi} \right)^2 \right). \quad (\text{B.4})$$

Then, the mode function X_L^c is defined as

$$\mathbf{X}_L^c(\vec{k}, \tau) = X_L^c(\vec{k}, \tau) a_{\vec{k}} + X_L^{c*}(\vec{k}, \tau) a_{-\vec{k}}^\dagger, \quad [a_{\vec{k}_1}, a_{\vec{k}_2}^\dagger] = (2\pi)^3 \delta^{(3)}(\vec{k}_1 - \vec{k}_2). \quad (\text{B.5})$$

Therefore, the equation of motion for the mode function is

$$X_L^{c''} + \left(k^2 + a^2 m_X^2 - \frac{k^2 \mathcal{H}^2}{k^2 + a^2 m_X^2} \left((n+2)(n+1) - 3(n+1)^2 \frac{a^2 m_X^2}{k^2 + a^2 m_X^2} \right) \right) X_L^c = 0, \quad (\text{B.6})$$

where $\mathcal{H} = aH$, and we assumed that $\phi \propto a^n$. Due to its complexity, this equation does not have an exact analytic solution. But the scales of \mathcal{H} , k , am_X are different in most eras, so one can solve this equation by only considering the dominant terms.

In the scenario in the main text, the $\phi \propto a^{2/5}$ for $a < a_{\text{tr}}$, and $\phi \sim \text{constant}$ for $a > a_{\text{tr}}$. So we approximate that $n = 2/5$ for $a < a_{\text{tr}}$, and $n = 0$ for $a > a_{\text{tr}}$. Also, the $a_{\text{nr}} > a_{\text{end}}$ is taken for the scenario in the main text, so the $\mathcal{H} \gg am_X$ is satisfied during the inflation. We can divide possible eras as in Tab. 5.

$(a-1) : k \gg \mathcal{H} \gg am_X, a < a_{\text{tr}}$	$(a-2) : k \gg \mathcal{H} \gg am_X, a > a_{\text{tr}}$
$(b-1) : \mathcal{H} \gg k \gg am_X, a < a_{\text{tr}}$	$(b-2) : \mathcal{H} \gg k \gg am_X, a > a_{\text{tr}}$
	$(c-2) : \mathcal{H} \gg am_X \gg k, a > a_{\text{tr}}$

Table 5: 5 possible eras for the evolution of longitudinal modes. We assume the Bunch-Davies initial condition [128], so the evolution of longitudinal mode starts from the $(a-1)$, and proceeds to the next era onto the down or right side. One can check that $(c-1) : \mathcal{H} \gg am_X \gg k, a < a_{\text{tr}}$ cannot occur in the scenario in the main text when $\alpha = 1$ and $\rho_X(a_0)/\rho_{\text{CDM}}(a_0) \sim 1$.

Since the observable scale of the universe should leave the horizon during inflation, the era at the end of inflation should be either $(b-2)$ or $(c-2)$. Therefore, possible cosmic histories during the inflation are

- $s_1: (a-1) \rightarrow (a-2) \rightarrow (b-2)$,

- s_2 : $(a-1) \rightarrow (a-2) \rightarrow (b-2) \rightarrow (c-2)$,
- s_3 : $(a-1) \rightarrow (b-1) \rightarrow (b-2)$,
- s_4 : $(a-1) \rightarrow (b-1) \rightarrow (b-2) \rightarrow (c-2)$.

Let's first solve Eq. (B.6) for $k \gg am_X$ case. This will give the general solution for the $(a-1)$, $(a-2)$, $(b-1)$, $(b-2)$. Using that $\mathcal{H} = -1/\tau$ ¹⁵, we get

$$X_L^{c''} + \left(k^2 + a^2 m_X^2 - \frac{1}{\tau^2} \left(\nu_\chi^2 - \frac{1}{4} \right) \right) X_L^c = 0, \quad \nu_\chi^2 = \begin{cases} \frac{361}{100} & (a < a_{\text{tr}}), \\ \frac{9}{4} & (a > a_{\text{tr}}). \end{cases} \quad (\text{B.7})$$

The solution is

$$X_L^c = \sqrt{-\tau} \left(C_{1,\nu_\chi} H_{\nu_\chi}^{(1)}(-k\tau) + C_{2,\nu_\chi} H_{\nu_\chi}^{(2)}(-k\tau) \right), \quad (\text{B.8})$$

where the $H^{(1)}(x)$ ($H^{(2)}(x)$) is the Hankel function of the first (second) kind, and C_{1,ν_χ} , C_{2,ν_χ} are undetermined coefficients for each ν_χ . We take the Bunch-Davies initial condition [128], so the longitudinal modes in the asymptotic past infinity is the plane wave solution as

$$X_L^c \sim \frac{1}{\sqrt{2k}} e^{-ik\tau}. \quad (\text{B.9})$$

This fixes the nonzero coefficients C_{1,ν_χ} for the outgoing solution and sets C_{2,ν_χ} to be zero. So the evolution of the longitudinal modes from the $(a-1)$ to $(b-1)$ is determined. In order to determine the evolution from the $(a-1)$ to $(a-2)$ or $(b-1)$ to $(b-2)$, one should connect each solutions at the a_{tr} as

$$C_{1,19/10} H_{19/10}^{(1)}(-k\tau)|_{\tau=\tau_{\text{tr}}^-} = C_{1,3/2} H_{3/2}^{(1)}(-k\tau)|_{\tau=\tau_{\text{tr}}^+}, \quad (\text{B.10})$$

where the LHS is the $(a-1)$ or $(b-1)$ solution, and RHS is the $(a-2)$ or $(b-2)$ solution applied at a_{tr} . Then one finds the following expressions for s_1 , and s_3 scenarios as

$$X_L^c(a_{\text{end}}) \sim \begin{cases} \frac{a_{\text{end}} H_{\text{inf}}}{\sqrt{2k^3}} & \text{for } s_1, \\ \frac{2^{19/10}}{\sqrt{2\pi}} \Gamma\left(\frac{19}{10}\right) \frac{(a_{\text{tr}} H_{\text{inf}})^{2/5}}{k^{2/5}} \frac{a_{\text{end}} H_{\text{inf}}}{\sqrt{2k^3}} & \text{for } s_3. \end{cases} \quad (\text{B.11})$$

One can calculate the solution at the $(c-2)$ by considering the evolution across the $k/a \sim m_X$ [85]. Let's denote the conformal time at the $k/a = m_X$ as a τ_* . Then, Eq. (B.6) becomes

$$X_L^{c''} + \left(k^2 \left(1 + \frac{\tau_*^2}{\tau^2} \right) - \frac{2\tau^2 - \tau_*^2}{(\tau^2 + \tau_*^2)^2} \right) X_L^c = 0. \quad (\text{B.12})$$

If $k\tau_*^2 < |\tau|$, one can approximate that

$$X_L^{c''} - \frac{2\tau^2 - \tau_*^2}{(\tau^2 + \tau_*^2)^2} X_L^c = 0. \quad (\text{B.13})$$

¹⁵The inflation ends at $\tau = 0$, and τ is negative during the inflation.

The solution to this equation is

$$X_L^c = D_1 \frac{1}{\sqrt{\tau^2 + \tau_*^2}} + D_2 \frac{\tau^2 + 3\tau\tau_*}{\sqrt{\tau^2 + \tau_*^2}}. \quad (\text{B.14})$$

Since the solution at $(b-2)$ is proportional to a ($\propto 1/\tau$), the $(b-2)$ solution has to be connected to the D_1 solution. Then one can determine D_2 by matching the $(b-2)$ and $(c-2)$ solutions at $\tau \gg \tau_*$. Now, if the $|\tau_*| \gg |\tau|$, Eq. (B.12) can be approximated as

$$X_L^{c''} + \left(k^2 \frac{\tau_*^2}{\tau^2} + \frac{1}{\tau^2} \right) X_L^c = 0. \quad (\text{B.15})$$

The solution to this equation is

$$X_L^c \sim \sqrt{-\tau} \left(a_1 J_{1/2} \left(\frac{\tau}{\tau_*} \right) + a_2 Y_{1/2} \left(\frac{\tau}{\tau_*} \right) \right) \sim E_1 \tau + E_2, \quad (\text{B.16})$$

where the $J_{1/2}$ is the Bessel function of the first kind, and $Y_{1/2}$ is the Bessel function of the second kind. The E_2 solution is connected to the D_1 solution, so one can actually use the D_1 solution of Eq. (B.13) to the end of inflation. An explicit calculation shows that

$$|X_L(a_{\text{end}})|^2 \sim \begin{cases} \frac{1}{2k^3} \frac{H_{\text{inf}}^2 k^2}{m_X^2(a_{\text{end}})} & \text{for } s_1, s_2, \\ \frac{2^{19/5}}{4\pi} \Gamma^2 \left(\frac{19}{10} \right) \frac{1}{k^3} \frac{(a_{\text{tr}} H_{\text{inf}})^{4/5}}{k^{4/5}} \frac{H_{\text{inf}}^2 k^2}{m_X^2(a_{\text{end}})} & \text{for } s_3, s_4, \end{cases} \quad (\text{B.17})$$

where the $X_L = X_L^c/g$, and, for all cases, the $|X_L|$ is constant on time close before the a_{end} . Then the power spectrum of \bar{X}_L is

$$\mathcal{P}_{\bar{X}_L}(a_{\text{end}}) \sim \begin{cases} \left(\frac{k H_{\text{inf}}}{2\pi a_{\text{end}} m_X(a_{\text{end}})} \right)^2 & \text{for } s_1, s_2, \\ \frac{2^{14/5}}{\pi} \Gamma^2 \left(\frac{19}{10} \right) \left(\frac{a_{\text{tr}} H_{\text{inf}}}{k} \right)^{4/5} \left(\frac{k H_{\text{inf}}}{2\pi a_{\text{end}} m_X(a_{\text{end}})} \right)^2 & \text{for } s_3, s_4. \end{cases} \quad (\text{B.18})$$

Here, the s_1, s_2 (s_3, s_4) corresponds to $a_{\text{tr}} < k/H_{\text{inf}}$ ($a_{\text{tr}} > k/H_{\text{inf}}$).

So, we found the solution of the X_L^c to the end of inflation for various cases. In order to find how these mode functions evolve after the inflation, it is convenient to use the redefined field $\bar{X}_L \equiv X_L/a$, and write the equation of motion with a cosmic time. Then, one can write the equation of motion of \bar{X}_L as

$$\begin{aligned} \ddot{\bar{X}}_L + \left(3H + \frac{2k^2}{k^2 + a^2 m_X^2} \left(H + \frac{\dot{\phi}}{\phi} \right) \right) \dot{\bar{X}}_L \\ + \left(a^2 m_X^2 + 2H^2 + \dot{H} + \frac{2k^2 H}{k^2 + a^2 m_X^2} \left(H + \frac{\dot{\phi}}{\phi} \right) \right) \bar{X}_L = 0. \end{aligned} \quad (\text{B.19})$$

Then for the super-horizon modes before the a_{nr} , the equation can be written as

$$\begin{cases} \ddot{\bar{X}}_L + (5 + 2n)H\dot{\bar{X}}_L + \frac{5 + 4n - 3w_b}{2} H^2 \bar{X}_L = 0 & \text{for } k/a \gg m_X, \\ \ddot{\bar{X}}_L + 3H\dot{\bar{X}}_L + \left(m_X^2 + \frac{1 - 3w_b}{2} H^2 \right) \bar{X}_L = 0 & \text{for } k/a \ll m_X, \end{cases} \quad (\text{B.20})$$

and the solution is given by

$$\bar{X}_L = \begin{cases} F_1 a^{-1} + F_2 a^{-(5+4n-3w_b)/2} & \text{for } k/a \gg m_X, \\ F_1 a^{-1} + F_2 a^{(3w_b-1)/2} & \text{for } k/a \ll m_X. \end{cases} \quad (\text{B.21})$$

Since the \bar{X}_L at the end of inflation is proportional to the a^{-1} , the F_1 solution becomes the same as the solution for the \bar{X} after the inflation. Therefore, the evolution of the longitudinal mode is the same as the homogeneous mode after the inflation.

References

- [1] PLANCK collaboration, *Planck 2018 results. VI. Cosmological parameters*, *Astron. Astrophys.* **641** (2020) A6 [[1807.06209](#)].
- [2] V. Silveira and A. Zee, *SCALAR PHANTOMS*, *Phys. Lett. B* **161** (1985) 136.
- [3] J. McDonald, *Gauge singlet scalars as cold dark matter*, *Phys. Rev. D* **50** (1994) 3637 [[hep-ph/0702143](#)].
- [4] C.P. Burgess, M. Pospelov and T. ter Veldhuis, *The Minimal model of nonbaryonic dark matter: A Singlet scalar*, *Nucl. Phys. B* **619** (2001) 709 [[hep-ph/0011335](#)].
- [5] A. Djouadi, O. Lebedev, Y. Mambrini and J. Quevillon, *Implications of LHC searches for Higgs–portal dark matter*, *Phys. Lett. B* **709** (2012) 65 [[1112.3299](#)].
- [6] A. Djouadi, A. Falkowski, Y. Mambrini and J. Quevillon, *Direct Detection of Higgs-Portal Dark Matter at the LHC*, *Eur. Phys. J. C* **73** (2013) 2455 [[1205.3169](#)].
- [7] Y. Mambrini, *Higgs searches and singlet scalar dark matter: Combined constraints from XENON 100 and the LHC*, *Phys. Rev. D* **84** (2011) 115017 [[1108.0671](#)].
- [8] A. Alves, S. Profumo and F.S. Queiroz, *The dark Z' portal: direct, indirect and collider searches*, *JHEP* **04** (2014) 063 [[1312.5281](#)].
- [9] O. Lebedev and Y. Mambrini, *Axial dark matter: The case for an invisible Z'* , *Phys. Lett. B* **734** (2014) 350 [[1403.4837](#)].
- [10] G. Arcadi, Y. Mambrini, M.H.G. Tytgat and B. Zaldivar, *Invisible Z' and dark matter: LHC vs LUX constraints*, *JHEP* **03** (2014) 134 [[1401.0221](#)].
- [11] G. Arcadi, Y. Mambrini and F. Richard, *Z-portal dark matter*, *JCAP* **03** (2015) 018 [[1411.2985](#)].
- [12] J. Ellis, A. Fowlie, L. Marzola and M. Raidal, *Statistical Analyses of Higgs- and Z-Portal Dark Matter Models*, *Phys. Rev. D* **97** (2018) 115014 [[1711.09912](#)].
- [13] M. Escudero, A. Berlin, D. Hooper and M.-X. Lin, *Toward (Finally!) Ruling Out Z and Higgs Mediated Dark Matter Models*, *JCAP* **12** (2016) 029 [[1609.09079](#)].
- [14] L.J. Hall, K. Jedamzik, J. March-Russell and S.M. West, *Freeze-In Production of FIMP Dark Matter*, *JHEP* **03** (2010) 080 [[0911.1120](#)].
- [15] G. Bhattacharyya, M. Dutra, Y. Mambrini and M. Pierre, *Freezing-in dark matter through a heavy invisible Z'* , *Phys. Rev. D* **98** (2018) 035038 [[1806.00016](#)].
- [16] K. Kaneta, Z. Kang and H.-S. Lee, *Right-handed neutrino dark matter under the $B - L$ gauge interaction*, *JHEP* **02** (2017) 031 [[1606.09317](#)].
- [17] K. Kaneta, H.-S. Lee and S. Yun, *Portal Connecting Dark Photons and Axions*, *Phys. Rev. Lett.* **118** (2017) 101802 [[1611.01466](#)].
- [18] P. Anastasopoulos, K. Kaneta, Y. Mambrini and M. Pierre, *Energy-momentum portal to dark matter and emergent gravity*, *Phys. Rev. D* **102** (2020) 055019 [[2007.06534](#)].

- [19] P. Brax, K. Kaneta, Y. Mambrini and M. Pierre, *Disformal dark matter*, *Phys. Rev. D* **103** (2021) 015028 [2011.11647].
- [20] P. Brax, K. Kaneta, Y. Mambrini and M. Pierre, *Metastable Conformal Dark Matter*, *Phys. Rev. D* **103** (2021) 115016 [2103.02615].
- [21] K. Kaneta, P. Ko and W.-I. Park, *Conformal portal to dark matter*, *Phys. Rev. D* **104** (2021) 075018 [2106.01923].
- [22] D. Chowdhury, E. Dudas, M. Dutra and Y. Mambrini, *Moduli Portal Dark Matter*, *Phys. Rev. D* **99** (2019) 095028 [1811.01947].
- [23] A. Kamada, K. Kaneta, K. Yanagi and H.-B. Yu, *Self-interacting dark matter and muon $g - 2$ in a gauged $U(1)_{L_\mu - L_\tau}$ model*, *JHEP* **06** (2018) 117 [1805.00651].
- [24] H.E.S. Velten, R.F. vom Marttens and W. Zimdahl, *Aspects of the cosmological “coincidence problem”*, *The European Physical Journal C* **74** (2014) .
- [25] H. Ooguri, E. Palti, G. Shiu and C. Vafa, *Distance and de Sitter Conjectures on the Swampland*, *Phys. Lett. B* **788** (2019) 180 [1810.05506].
- [26] S.K. Garg and C. Krishnan, *Bounds on Slow Roll and the de Sitter Swampland*, *JHEP* **11** (2019) 075 [1807.05193].
- [27] PLANCK collaboration, *Planck 2018 results. VI. Cosmological parameters*, *Astron. Astrophys.* **641** (2020) A6 [1807.06209].
- [28] A.G. Riess et al., *A Comprehensive Measurement of the Local Value of the Hubble Constant with 1 km/s/Mpc Uncertainty from the Hubble Space Telescope and the SH0ES Team*, *Astrophys. J. Lett.* **934** (2022) L7 [2112.04510].
- [29] L. Verde, T. Treu and A.G. Riess, *Tensions between the Early and the Late Universe*, *Nature Astron.* **3** (2019) 891 [1907.10625].
- [30] E. Di Valentino, O. Mena, S. Pan, L. Visinelli, W. Yang, A. Melchiorri et al., *In the realm of the Hubble tension—a review of solutions*, *Class. Quant. Grav.* **38** (2021) 153001 [2103.01183].
- [31] L. Perivolaropoulos and F. Skara, *Challenges for Λ CDM: An update*, *New Astron. Rev.* **95** (2022) 101659 [2105.05208].
- [32] E. Di Valentino, *Challenges of the Standard Cosmological Model*, *Universe* **8** (2022) 399.
- [33] N. Schöneberg, G. Franco Abellán, A. Pérez Sánchez, S.J. Witte, V. Poulin and J. Lesgourgues, *The H_0 Olympics: A fair ranking of proposed models*, *Phys. Rept.* **984** (2022) 1 [2107.10291].
- [34] E. Di Valentino, A. Melchiorri and O. Mena, *Can interacting dark energy solve the H_0 tension?*, *Phys. Rev. D* **96** (2017) 043503 [1704.08342].
- [35] W. Yang, S. Pan, E. Di Valentino, R.C. Nunes, S. Vagnozzi and D.F. Mota, *Tale of stable interacting dark energy, observational signatures, and the H_0 tension*, *JCAP* **09** (2018) 019 [1805.08252].
- [36] V. Poulin, T.L. Smith, T. Karwal and M. Kamionkowski, *Early Dark Energy Can Resolve The Hubble Tension*, *Phys. Rev. Lett.* **122** (2019) 221301 [1811.04083].
- [37] S. Vagnozzi, *New physics in light of the H_0 tension: An alternative view*, *Phys. Rev. D* **102** (2020) 023518 [1907.07569].
- [38] E. Di Valentino, A. Melchiorri, O. Mena and S. Vagnozzi, *Interacting dark energy in the early 2020s: A promising solution to the H_0 and cosmic shear tensions*, *Phys. Dark Univ.* **30** (2020) 100666 [1908.04281].

- [39] E. Di Valentino, A. Melchiorri, O. Mena and S. Vagnozzi, *Nonminimal dark sector physics and cosmological tensions*, *Phys. Rev. D* **101** (2020) 063502 [[1910.09853](#)].
- [40] K. Jedamzik, L. Pogosian and G.-B. Zhao, *Why reducing the cosmic sound horizon alone can not fully resolve the Hubble tension*, *Commun. in Phys.* **4** (2021) 123 [[2010.04158](#)].
- [41] G. Choi, T.T. Yanagida and N. Yokozaki, *A model of interacting dark matter and dark radiation for H_0 and σ_8 tensions*, *JHEP* **01** (2021) 127 [[2010.06892](#)].
- [42] M.G. Dainotti, B. De Simone, T. Schiavone, G. Montani, E. Rinaldi and G. Lambiase, *On the Hubble constant tension in the SNe Ia Pantheon sample*, *Astrophys. J.* **912** (2021) 150 [[2103.02117](#)].
- [43] S. Vagnozzi, *Consistency tests of Λ CDM from the early integrated Sachs-Wolfe effect: Implications for early-time new physics and the Hubble tension*, *Phys. Rev. D* **104** (2021) 063524 [[2105.10425](#)].
- [44] E. Mawas, L. Street, R. Gass and L.C.R. Wijewardhana, *Interacting dark energy axions in light of the Hubble tension*, [2108.13317](#).
- [45] M.G. Dainotti, B. De Simone, T. Schiavone, G. Montani, E. Rinaldi, G. Lambiase et al., *On the Evolution of the Hubble Constant with the SNe Ia Pantheon Sample and Baryon Acoustic Oscillations: A Feasibility Study for GRB-Cosmology in 2030*, *Galaxies* **10** (2022) 24 [[2201.09848](#)].
- [46] Y.-H. Yao and X.-H. Meng, *Can interacting dark energy with dynamical coupling resolve the Hubble tension*, *Phys. Dark Univ.* **39** (2023) 101165.
- [47] Y. Zhai, W. Giarè, C. van de Bruck, E. Di Valentino, O. Mena and R.C. Nunes, *A Consistent View of Interacting Dark Energy from Multiple CMB Probes*, [2303.08201](#).
- [48] C. Wetterich, *Cosmology and the Fate of Dilatation Symmetry*, *Nucl. Phys. B* **302** (1988) 668 [[1711.03844](#)].
- [49] B. Ratra and P.J.E. Peebles, *Cosmological Consequences of a Rolling Homogeneous Scalar Field*, *Phys. Rev. D* **37** (1988) 3406.
- [50] R.R. Caldwell, R. Dave and P.J. Steinhardt, *Cosmological imprint of an energy component with general equation of state*, *Phys. Rev. Lett.* **80** (1998) 1582 [[astro-ph/9708069](#)].
- [51] I. Zlatev, L.-M. Wang and P.J. Steinhardt, *Quintessence, cosmic coincidence, and the cosmological constant*, *Phys. Rev. Lett.* **82** (1999) 896 [[astro-ph/9807002](#)].
- [52] L. Pilo, D.A.J. Rayner and A. Riotto, *Gauge quintessence*, *Phys. Rev. D* **68** (2003) 043503 [[hep-ph/0302087](#)].
- [53] A. Mehrabi, A. Maleknejad and V. Kamali, *Gaugessence: a dark energy model with early time radiation-like equation of state*, *Astrophys. Space Sci.* **362** (2017) 53 [[1510.00838](#)].
- [54] A.S. Gevorkyan, *Quantum Vacuum: The Structure of Empty Space-Time and Quintessence with Gauge Symmetry Group $SU(2) \otimes U(1)$* , *Particles* **2** (2019) 281 [[1807.06932](#)].
- [55] C.T. Hill and A.K. Leibovich, *Natural Theories of Ultralow Mass PNGB's: Axions and Quintessence*, *Phys. Rev. D* **66** (2002) 075010 [[hep-ph/0205237](#)].
- [56] J.-A. Gu and W.-Y.P. Hwang, *Can the quintessence be a complex scalar field?*, *Phys. Lett. B* **517** (2001) 1 [[astro-ph/0105099](#)].
- [57] L.A. Boyle, R.R. Caldwell and M. Kamionkowski, *Spintessence! New models for dark matter and dark energy*, *Phys. Lett. B* **545** (2002) 17 [[astro-ph/0105318](#)].
- [58] X.-z. Li, J.-g. Hao and D.-j. Liu, *Quintessence with $O(N)$ symmetry*, *Class. Quant. Grav.* **19** (2002) 6049 [[astro-ph/0107171](#)].

- [59] R. Mainini and S.A. Bonometto, *Dark matter and dark energy from the solution of the strong-CP problem*, *Phys. Rev. Lett.* **93** (2004) 121301 [[astro-ph/0406114](#)].
- [60] J.A. Frieman, C.T. Hill, A. Stebbins and I. Waga, *Cosmology with ultralight pseudo Nambu-Goldstone bosons*, *Phys. Rev. Lett.* **75** (1995) 2077 [[astro-ph/9505060](#)].
- [61] J.E. Kim, *Axion and almost massless quark as ingredients of quintessence*, *JHEP* **05** (1999) 022 [[hep-ph/9811509](#)].
- [62] K. Choi, *String or M theory axion as a quintessence*, *Phys. Rev. D* **62** (2000) 043509 [[hep-ph/9902292](#)].
- [63] J.E. Kim and H.P. Nilles, *A Quintessential axion*, *Phys. Lett. B* **553** (2003) 1 [[hep-ph/0210402](#)].
- [64] S.M. Carroll, *Quintessence and the rest of the world*, *Phys. Rev. Lett.* **81** (1998) 3067 [[astro-ph/9806099](#)].
- [65] M. Rinaldi, *Higgs Dark Energy*, *Class. Quant. Grav.* **32** (2015) 045002 [[1404.0532](#)].
- [66] M. Rinaldi, *Dark energy as a fixed point of the Einstein Yang-Mills Higgs Equations*, *JCAP* **10** (2015) 023 [[1508.04576](#)].
- [67] M. Álvarez, J.B. Orjuela-Quintana, Y. Rodriguez and C.A. Valenzuela-Toledo, *Einstein Yang-Mills Higgs dark energy revisited*, *Class. Quant. Grav.* **36** (2019) 195004 [[1901.04624](#)].
- [68] J.B. Orjuela-Quintana, M. Alvarez, C.A. Valenzuela-Toledo and Y. Rodriguez, *Anisotropic Einstein Yang-Mills Higgs Dark Energy*, *JCAP* **10** (2020) 019 [[2006.14016](#)].
- [69] E. Di Valentino, A. Melchiorri and J. Silk, *Reconciling Planck with the local value of H_0 in extended parameter space*, *Phys. Lett. B* **761** (2016) 242 [[1606.00634](#)].
- [70] S. Joudaki, M. Kaplinghat, R. Keeley and D. Kirkby, *Model independent inference of the expansion history and implications for the growth of structure*, *Phys. Rev. D* **97** (2018) 123501 [[1710.04236](#)].
- [71] E.O. Colgáin and H. Yavartanoo, *Testing the Swampland: H_0 tension*, *Phys. Lett. B* **797** (2019) 134907 [[1905.02555](#)].
- [72] L. Heisenberg, H. Villarrubia-Rojo and J. Zosso, *Simultaneously solving the H_0 and σ_8 tensions with late dark energy*, [2201.11623](#).
- [73] L. Heisenberg, H. Villarrubia-Rojo and J. Zosso, *Can late-time extensions solve the H_0 and σ_8 tensions?*, *Phys. Rev. D* **106** (2022) 043503 [[2202.01202](#)].
- [74] B.-H. Lee, W. Lee, E.O. Colgáin, M.M. Sheikh-Jabbari and S. Thakur, *Is local H_0 at odds with dark energy EFT?*, *JCAP* **04** (2022) 004 [[2202.03906](#)].
- [75] A. Banerjee, H. Cai, L. Heisenberg, E.O. Colgáin, M.M. Sheikh-Jabbari and T. Yang, *Hubble sinks in the low-redshift swampland*, *Phys. Rev. D* **103** (2021) L081305 [[2006.00244](#)].
- [76] K. Kaneta, H.-S. Lee, J. Lee and J. Yi, *Gauged quintessence*, *Journal of Cosmology and Astroparticle Physics* **2023** (2023) 005.
- [77] Y.-H. Yao and X.-H. Meng, *Can interacting dark energy with dynamical coupling resolve the Hubble tension*, [2207.05955](#).
- [78] J. Preskill, M.B. Wise and F. Wilczek, *Cosmology of the Invisible Axion*, *Phys. Lett. B* **120** (1983) 127.
- [79] L.F. Abbott and P. Sikivie, *A Cosmological Bound on the Invisible Axion*, *Phys. Lett. B* **120** (1983) 133.
- [80] M. Dine and W. Fischler, *The Not So Harmless Axion*, *Phys. Lett. B* **120** (1983) 137.
- [81] J.E. Kim, *Light Pseudoscalars, Particle Physics and Cosmology*, *Phys. Rept.* **150** (1987) 1.

- [82] A.E. Nelson and J. Scholtz, *Dark Light, Dark Matter and the Misalignment Mechanism*, *Phys. Rev. D* **84** (2011) 103501 [[1105.2812](#)].
- [83] P.W. Graham, J. Mardon and S. Rajendran, *Vector Dark Matter from Inflationary Fluctuations*, *Phys. Rev. D* **93** (2016) 103520 [[1504.02102](#)].
- [84] P. Arias, D. Cadamuro, M. Goodsell, J. Jaeckel, J. Redondo and A. Ringwald, *WISPy Cold Dark Matter*, *JCAP* **06** (2012) 013 [[1201.5902](#)].
- [85] K. Nakayama, *Vector Coherent Oscillation Dark Matter*, *JCAP* **10** (2019) 019 [[1907.06243](#)].
- [86] G. Alonso-Álvarez, T. Hogle and J. Jaeckel, *Misalignment \mathcal{E} Co.: (Pseudo-)scalar and vector dark matter with curvature couplings*, *JCAP* **02** (2020) 014 [[1905.09836](#)].
- [87] K. Nakayama, *Constraint on Vector Coherent Oscillation Dark Matter with Kinetic Function*, *JCAP* **08** (2020) 033 [[2004.10036](#)].
- [88] P.J. Steinhardt, L.-M. Wang and I. Zlatev, *Cosmological tracking solutions*, *Phys. Rev. D* **59** (1999) 123504 [[astro-ph/9812313](#)].
- [89] J. Martin, *Quintessence: a mini-review*, *Mod. Phys. Lett. A* **23** (2008) 1252 [[0803.4076](#)].
- [90] S. Tsujikawa, *Quintessence: A Review*, *Class. Quant. Grav.* **30** (2013) 214003 [[1304.1961](#)].
- [91] P. Brax and J. Martin, *The Robustness of quintessence*, *Phys. Rev. D* **61** (2000) 103502 [[astro-ph/9912046](#)].
- [92] M. Doran and J. Jaeckel, *Loop corrections to scalar quintessence potentials*, *Phys. Rev. D* **66** (2002) 043519 [[astro-ph/0203018](#)].
- [93] J.A. Casas, J. Garcia-Bellido and M. Quiros, *Scalar - tensor theories of gravity with phi dependent masses*, *Class. Quant. Grav.* **9** (1992) 1371 [[hep-ph/9204213](#)].
- [94] J. Garcia-Bellido, *Dark matter with variable masses*, *Int. J. Mod. Phys. D* **2** (1993) 85 [[hep-ph/9205216](#)].
- [95] G.W. Anderson and S.M. Carroll, *Dark matter with time dependent mass*, in *1st International Conference on Particle Physics and the Early Universe*, pp. 227–229, 9, 1997, DOI [[astro-ph/9711288](#)].
- [96] R. Fardon, A.E. Nelson and N. Weiner, *Dark energy from mass varying neutrinos*, *JCAP* **10** (2004) 005 [[astro-ph/0309800](#)].
- [97] A. Berlin and D. Hooper, *Axion-Assisted Production of Sterile Neutrino Dark Matter*, *Phys. Rev. D* **95** (2017) 075017 [[1610.03849](#)].
- [98] H. Davoudiasl and G. Mohlabeng, *Getting a THUMP from a WIMP*, *JHEP* **04** (2020) 177 [[1912.05572](#)].
- [99] L. Boubekour and S. Profumo, *Tremaine-Gunn limit with mass-varying particles*, *Phys. Rev. D* **107** (2023) 103535 [[2302.10246](#)].
- [100] Y. ChoeJo, Y. Kim and H.-S. Lee, *Dirac-Majorana neutrino type conversion induced by an oscillating scalar dark matter*, [2305.16900](#).
- [101] K. Kaneta and K.-y. Oda, *Non-thermal Higgs Spectrum in Reheating Epoch: Primordial Condensate vs. Stochastic Fluctuation*, [2304.12578](#).
- [102] G. Wentzel, *Eine verallgemeinerung der quantenbedingungen für die zwecke der wellenmechanik*, *Zeitschrift für Physik* **38** (1926) 518.
- [103] H.A. Kramers, *Wellenmechanik und halbzahlige quantisierung*, *Zeitschrift für Physik* **39** (1926) 828.
- [104] L. Brillouin, *La mécanique ondulatoire de Schrödinger; une méthode générale de resolution par approximations successives*, *Compt. Rend. Hebd. Seances Acad. Sci.* **183** (1926) 24.

- [105] D. Wands, K.A. Malik, D.H. Lyth and A.R. Liddle, *A New approach to the evolution of cosmological perturbations on large scales*, *Phys. Rev. D* **62** (2000) 043527 [[astro-ph/0003278](#)].
- [106] M. Kawasaki, K. Nakayama, T. Sekiguchi, T. Suyama and F. Takahashi, *Non-Gaussianity from isocurvature perturbations*, *JCAP* **11** (2008) 019 [[0808.0009](#)].
- [107] D. Langlois, F. Vernizzi and D. Wands, *Non-linear isocurvature perturbations and non-Gaussianities*, *JCAP* **12** (2008) 004 [[0809.4646](#)].
- [108] D.H. Lyth, K.A. Malik and M. Sasaki, *A General proof of the conservation of the curvature perturbation*, *JCAP* **05** (2005) 004 [[astro-ph/0411220](#)].
- [109] PLANCK collaboration, *Planck 2018 results. X. Constraints on inflation*, *Astron. Astrophys.* **641** (2020) A10 [[1807.06211](#)].
- [110] M. Malquarti and A.R. Liddle, *Initial conditions for quintessence after inflation*, *Phys. Rev. D* **66** (2002) 023524 [[astro-ph/0203232](#)].
- [111] J. Martin and M.A. Musso, *Stochastic quintessence*, *Phys. Rev. D* **71** (2005) 063514 [[astro-ph/0410190](#)].
- [112] A.i. Starobinsky, *Fundamental interactions*, *Phys., Moscow, MGPI* (1984) 55.
- [113] A. Starobinsky, *Field theory, quantum gravity, and strings*, *Lecture Notes in Phys.* **246** (1986) 107.
- [114] V. Iršič, M. Viel, M.G. Haehnelt, J.S. Bolton and G.D. Becker, *First constraints on fuzzy dark matter from Lyman- α forest data and hydrodynamical simulations*, *Phys. Rev. Lett.* **119** (2017) 031302 [[1703.04683](#)].
- [115] T. Kobayashi, R. Murgia, A. De Simone, V. Iršič and M. Viel, *Lyman- α constraints on ultralight scalar dark matter: Implications for the early and late universe*, *Phys. Rev. D* **96** (2017) 123514 [[1708.00015](#)].
- [116] L. Hui, *Wave Dark Matter*, *Ann. Rev. Astron. Astrophys.* **59** (2021) 247 [[2101.11735](#)].
- [117] A. Arvanitaki, S. Dimopoulos, S. Dubovsky, N. Kaloper and J. March-Russell, *String Axiverse*, *Phys. Rev. D* **81** (2010) 123530 [[0905.4720](#)].
- [118] A. Arvanitaki and S. Dubovsky, *Exploring the String Axiverse with Precision Black Hole Physics*, *Phys. Rev. D* **83** (2011) 044026 [[1004.3558](#)].
- [119] P. Pani, V. Cardoso, L. Gualtieri, E. Berti and A. Ishibashi, *Black hole bombs and photon mass bounds*, *Phys. Rev. Lett.* **109** (2012) 131102 [[1209.0465](#)].
- [120] R. Brito, V. Cardoso and P. Pani, *Superradiance: New Frontiers in Black Hole Physics*, *Lect. Notes Phys.* **906** (2015) pp.1 [[1501.06570](#)].
- [121] M. Baryakhtar, R. Lasenby and M. Teo, *Black Hole Superradiance Signatures of Ultralight Vectors*, *Phys. Rev. D* **96** (2017) 035019 [[1704.05081](#)].
- [122] H. Davoudiasl and P.B. Denton, *Ultralight Boson Dark Matter and Event Horizon Telescope Observations of M87**, *Phys. Rev. Lett.* **123** (2019) 021102 [[1904.09242](#)].
- [123] K. Choi, S.H. Im and C.S. Shin, *Recent Progress in the Physics of Axions and Axion-Like Particles*, *Ann. Rev. Nucl. Part. Sci.* **71** (2021) 225 [[2012.05029](#)].
- [124] N. Arkani-Hamed, L. Motl, A. Nicolis and C. Vafa, *The String landscape, black holes and gravity as the weakest force*, *JHEP* **06** (2007) 060 [[hep-th/0601001](#)].
- [125] B. Heidenreich, M. Reece and T. Rudelius, *Evidence for a sublattice weak gravity conjecture*, *JHEP* **08** (2017) 025 [[1606.08437](#)].
- [126] B. Heidenreich, M. Reece and T. Rudelius, *The Weak Gravity Conjecture and Emergence from an Ultraviolet Cutoff*, *Eur. Phys. J. C* **78** (2018) 337 [[1712.01868](#)].

- [127] N. Kitajima and K. Nakayama, *Viable Vector Coherent Oscillation Dark Matter*, [2303.04287](#).
- [128] T.S. Bunch and P.C.W. Davies, *Quantum Field Theory in de Sitter Space: Renormalization by Point Splitting*, *Proc. Roy. Soc. Lond. A* **360** (1978) 117.